International Journal of Environmental Science and Technology (2023) 20:31–40
https://doi.org/10.1007/s13762-022-04030-0

ORIGINAL PAPER

One-nanometre-resolution evidence of As(III) anoxic and oxic transformations on the surfaces of expandable clay minerals

J. Cervini-Silva[1] · E. Palacios[2] · A. Nieto-Camacho[3] · L. C. S. Peña[4] · L. M. del Razo[4]

Received: 19 May 2021 / Revised: 6 December 2021 / Accepted: 10 February 2022 / Published online: 19 March 2022

Abstract

Arsenic (As) is a priority pollutant found in water bodies, sediments and soils; therefore, mineral surfaces are critical for the environmental distribution of this element. The objective of this work was to analyse expandable clay minerals [hectorite (Fe-poor) and nontronite (Fe-rich)] exposed to As [as As(III), the most toxic form of As; 10^{-4} M sodium arsenite in water, $pH_0 = 7.2$, 25 ± 1 °C] with 1 nm precision using hydride generation–cryotrapping–atomic absorption spectrometry, high-resolution scanning electron microscopy and energy-dispersive spectrometry. In supernatant solutions, As(III) underwent no transformation. The accumulation of As(III) was registered in hectorite (4%) and nontronite (2.7%). The outcome of this work expanded on current knowledge on the interaction between As(III) and expandable clay minerals. The higher content of structural Fe in nontronite vs. hectorite favoured the retention of As(III). Arguably, adsorbed As(III) on nontronite surfaces (1) transformed to arsenical ferrihydrite or (2) bonded with naturally occurring S; both processes facilitated its nonreversible surface bonding. In addition, adsorbed As(III) on nontronite and hectorite surfaces reversibly bonded to surface O.

Keywords Available vs non-available As · Arsenopyrite · Ferrihydrite · Hectorite · Nontronite

Introduction

Arsenic (As) is a priority environmental pollutant. According to the World Health Organization, the concentration of this element in drinking water should not exceed 10 µg L^{-1} (Smedley and Kinniburgh 2002). An alternative technology to remove this metalloid from water matrices consists of using minerals. A study conducted in discharged water in a contaminated industrial site showed that 1–10 µm euhedral crystals of pyrite (FeS_2) adsorbed and co-precipitated As, and the mineral retained up to 500–4000 mg/kg As (Saunders et al. 2018). In addition, accompanying bench experiments under strict anoxic conditions confirmed that the retention of As(III) (dissolved As_2O_3) on the mineral surfaces (crushed to several size fractions) increased with decreasing proton activity ($5 < pH$).

Ubiquitously found in the environment are clays, which are inorganic materials ≤ 2 µm, composed of clay minerals, i.e. specific minerals that mainly occur in the clay size fraction of the soil (e.g. kaolinite, illite, montmorillonite, smectite; Moore and Reynolds 1989). Despite its importance, the adsorption of As in its most toxic form, i.e., As(III), is far from being understood and remains an unresolved topic (Table 1 after Fendorf et al., 2010b). Thus, the present study addresses this complex but unresolved topic. A preceding study reported the adsorption envelopes, and the corresponding constant capacitance model calculations for As(III) adsorption on amorphous Al and Fe (surface areas 660 and 350 m^2 g^{-1}), kaolinite (KGa-2, 21.6 m^2 g^{-1}), montmorillonite (SAz-1, 68.9 m^2 g^{-1}) and illite (IMt-2, 22.6 m^2 g^{-1}) showed maximum values of

Editorial responsibility: Babatunde Femi Bakare.

✉ J. Cervini-Silva
jcervini@correo.cua.uam.mx

[1] Departamento de Procesos Y Tecnología, División de Ciencias Naturales E Ingeniería, Universidad Autónoma Metropolitana, Unidad Cuajimalpa, Prol. Vasco de Quiroga 4871, Col. Santa Fe, Del Cuajimalpa de Morelos Ciudad de México, C.P. 05348 Ciudad de México, México

[2] Departamento de Microscopía Electrónica, Instituto Mexicano del Petróleo, Ciudad de México, México

[3] Laboratorio de Pruebas Biológicas, Instituto de Química, Universidad Nacional Autónoma de México, Ciudad de México, México

[4] Departamento de Toxicología, Centro de Investigación Y de Estudios Avanzados del Instituto Politécnico Nacional, Ciudad de México, México

17 µmol g^{-1} ($7 \leq pH \leq 9$), ca. 40 µmol g^{-1} ($2 \leq pH \leq 11$), 0.27 µmol g^{-1} ($8 \leq pH \leq 10$), 0.2 µmol g^{-1} ($7.5 \leq pH \leq 9.5$) and 0.25 µmol g^{-1} ($7.5 \leq pH \leq 9.5$; Goldberg 2002). That study also fitted data to the constant capacitance model, and the adsorption of As on am-Fe oxide and illite quantitatively fit. However, the fitting of the model to the adsorption on am-Al oxide and kaolinite was underpredicted and overpredicted compared to the experimental values at $7 \leq pH \leq 9$, respectively. Finally, in that study, the adsorption of As was attributed to inner-sphere surface complexation, while fitting of the model was not attempted for data corresponding to montmorillonite.

Far-from-equilibrium experiments to assess the sorption of As(III) on clay mineral surfaces [kaolinite (KGa-1), montmorillonite (SWy-1) and nontronite (iron-rich clay mineral, NAu-1 and NAu-2; Ghorbanzadeh et al. 2015)] showed that the sorption kinetics were described by pseudo-second-order equations. Based on the high values of the r^2 coefficients, the adsorption behaviour was well described by Freundlich isotherms for all clays except kaolinite. The authors of that study concluded that nontronite NAu-1 was the most effective clay for removing As(III) from solutions (rate constant ca. 0.056 g mg^{-1} min^{-1}; Ghorbanzadeh et al. 2015).

High-resolution scanning electron microscopy and energy-dispersive spectrometry (HRSEM EDS). Clay minerals are composed of assemblages of tetrahedral and octahedral sheets, whereby the tetrahedral Si–O and O–O bond distances are approximately 0.162 nm and 0.264 nm, respectively, and the Al octahedral O–O and OH–OH distances are 0.267 nm and 0.294 nm, respectively (Sparks 2003, p. 51). Here, the authors studied the atomic environment of As(III) on clay mineral surfaces with 1 nm precision using HRSEM–EDS. This experimental approach guaranteed results with high accuracy, especially if the mineral As concentrations were low to very low. The outcome of this study well complemented reports on the atomic environment of As on mineral surfaces determined by wet chemistry, computational modelling and X-ray absorption near edge spectroscopy [XANES; high energy resolution (< 0.5 eV) and high spatial resolution (100 µm); (Bostick and Fendorf 2003; Sverjensky and Fukushi 2006; Fendorf et al. 2010a)]. Unveiling the atomic environments of mineral As and bond energies that control the release of As into the solution with high precision will help predict the fate of this metalloid in aquifers, particularly in those containing low to very low amounts of organic carbon. Then, the cycling of the elements can be regulated by the chemistry of the minerals (Fendorf et al. 2010b).

The HRSEM–EDS analysis was complemented with hydride generation–cryotrapping–atomic absorption spectrometry (HG-CT-AAS) analysis. Taken together, these techniques enabled us to achieve low detection limit analyses of both supernatant solutions and surfaces. The work was conducted at the referred institutions on June 2019.

Materials and methods

Expandable clay minerals

Hectorite {SHCa-1; $(Na)_{0.80}[Si_{7.90}Al_{0.1}][Mg_{5.30}Li_{0.70}]O_{20}(OH)_4$; Hector, California, USA; 50% hectorite, 43% calcite, 3% quartz, 3% dolomite (Chipera and Bish 2001), 0.32% Fe_2O_3 with no detectable Fe^{2+} (Mermut and Cano 2001; Środoń and McCarty 2008)} and nontronite {NAu-1; $(Na_{1.05}[Si_{6.98}Al_{0.95}Fe_{0.07}][Al_{0.36}Fe_{3.61}Mg_{0.04}]O_{20}(OH)_4$; Uley Mine, Australia; nontronite and trace amounts of feldspar and quartz (Keeling et al. 2000)} were purchased from the repository of the clay minerals society and used as received.

Reaction between As(III) and expandable clay minerals (hectorite and nontronite)

The source of As(III) was sodium (meta)arsenite (Merck CAS Number 7784–46-5; ≤ 90%). A solution of 10^{-4} M sodium arsenite in water ($pH_0 = 7.2$) was prepared. Then, 10 mL of the resulting solution was added to 1 g of clay mineral and allowed to react at room temperature (25 ± 1 °C) for 1 week. Solids were recovered, placed in Teflon weighing plates, covered with Parafilm, allowed to dry under ambient conditions for a week, and finally prepared for microscopic analysis (Sect. 2.4).

HG-CT-AAS

Arsenic species in supernatant solutions were analysed by HG-CT-AAS, which enables the quantification of seven arsenic species, including arsenite, arsenate, methylarsenite, methylarsenate, dimethylarsenite, dimethylarsenate and trimethylarsine oxide (Supplementary material after Del Razo et al. 2001; Devesa et al. 2004; Hernández-Zavala et al. 2008).

HRSEM–EDS

The clay mineral samples were placed in an Al sample holder, fixed with carbon tape, and analysed by HRSEM. We used an environmental scanning electron microscope Philips XL30 ESEM (amplification range 10–200,000×; resolution 3.5 nm) and a solid-state energy-dispersive spectrometer equipped with an X-ray Si (Li) ultrathin window to detect elements from Be and onwards.

Results and discussion

As in supernatant solutions

As evidenced by HG-CT-AAS, As(III) in the solution showed no or below-detection-limit transformation to As(V),

Table 1 Retention maxima from adsorption isotherms at fixed pH and adsorption envelopes for As(III) on various solids[a]

Adsorbent	As(III) mmole kg^{-1}	pH	$As(III)_{aq}$[b]/$As(III)_{ads}$[c]	pH_{max}[d]
Al oxides				
Activated alumina	14	6.5–8.5	26; 11(8.2)	3–10
Bauxite	16	6.5–8.5	16; 9(8.5)	3–10
Amorphous Al hydroxide	–	–	20; 16(8.5)	7–9.5
Aluminosilicates				
Montmorillonite	3	5.0	20; 0.4(3)	3–4
Kaolinite	1	5.0	20; 0.25 (8–10)	7–11
Illite	–	–	20; 0.22 (8–9)	7–10
Fe (hydr)oxides				
Hydrous ferric oxide	2675	8.0	20; 40 (2–11)	2–11
			100; 1500 (8–9)	5–9.5
Goethite	173	8	100; 120 (8–9)	4–10
Magnetite	332	8	100; 140 (9.0)	8–9.5
2-line ferrihydrite	≥6000	4.6	–	–
2-line ferrihydrite on sand	1206	7.1	–	–
Humic acids	–	–	20; 110 (8)	7–9

[a]Data taken from Tables 1 and 2 in Fendorf et al. 2010b

[b]Initial aqueous concentration (μM)

[c]Maximum adsorption (mmole kg^{-1}) at indicated pH

[d]pH range over which maximum adsorption occurred

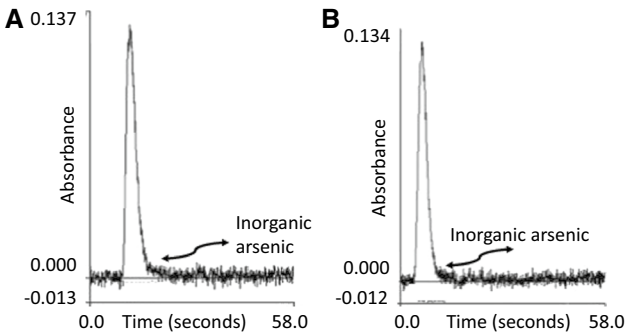

Fig. 1 Retention of As(III) in the clay minerals

while its concentration decreased upon exposure to clay minerals (Fig. 1).

Characteristic equations

As determined by the EDS analysis, the clay minerals were primarily composed of Si, O, Fe, Al, As, S (%atom; Table 2) and other elements (footnotes in Table 2).

The elemental associations were determined by calculating the ratios As/S, Fe/S, As/O, Fe/O, Si/O, Al/O, As/Fe, and Al/Fe; then, the ratios were plotted for comparison (Table 3; Figs. 2, 3, 4 and 5). Data within precision were considered, and outliers were discarded.

Unlike for hectorite, the surface analysis of nontronite confirmed the As accumulation, which was related to compositional and structural units. %As increased with %Fe (Fig. 2):

$$\{\%\mathrm{As}\} = 0.099\,\{\%\mathrm{Fe}\}^2 - 0.09\{\%\mathrm{Fe}\} + 0.65, r^2 = 0.93 \quad (1)$$

Additionally, the data trends of As/O, As/S, Fe/O and Fe/S were related, as described by Eqs. 2 and 3 (Figs. 3, 4):

$$\{\mathrm{As}/S\} = 0.17\{\mathrm{Fe}/S\}^2 - 0.11\{\mathrm{Fe}/S\} + 0.43, r^2 = 0.95 \quad (2)$$

$$\{\mathrm{As}/O\} = 0.35\{\mathrm{Fe}/O\}^2 - 0.07\{\mathrm{Fe}/O\} + 0.01, r^2 = 0.93 \quad (3)$$

Notably, the fitting coefficients of Eqs. 1, 2 and 3 were similar; however, a direct comparison of the polynomial coefficients showed that Fe/O served as a good predictor for the As accumulation, surpassing %Fe and Fe/S. Additionally, a positive, shallower relation was found to hold true between the data trends of As/Fe and Al/Fe (Eq. 4 after Fig. 5). Finally, no relation held true between the Si content and the As accumulation (Tables 2 and 3).

$$\{\mathrm{As/Fe}\} = -0.0017\{\mathrm{Al/Fe}\}^2 + 0.0502\{\mathrm{Al/Fe}\} + 0.0498, r^2 = 0.83 \quad (4)$$

Table 2 EDS analyses of the clay minerals reacted with As(III)

	As	Fe	Al	S	O	Si
Nontronite NAu-1[a]						
S1	1.4 ± 0.3	13 ± 1	8.5 ± 1.3	1.2 ± 0.5	58 ± 9	15 ± 2
S2	0.7 ± 0.1	11 ± 1	5.3 ± 0.7	1.8 ± 0.4	42 ± 6	14 ± 1
S3	0.6 ± 0.1	7.3 ± 0.4	6.7 ± 0.8	1.7 ± 0.4	49 ± 7	13 ± 1
S4	0.6 ± 0.1	10 ± 1	4.2 ± 0.6	2.5 ± 0.4	40 ± 6	16 ± 1
S5	0.9 ± 0.2	12 ± 1	6.3 ± 0.9	2.4 ± 0.6	38 ± 6	14 ± 1
S6	0.6 ± 0.1	5.1 ± 0.4	8.2 ± 0.9	2.1 ± 0.3	41 ± 6	11 ± 1
S7	0.7 ± 0.1	11 ± 1	7.9 ± 0.9	3.2 ± 0.5	45 ± 6	20 ± 2
S8	0.5 ± 0.07	5.9 ± 0.3	5.6 ± 0.6	2.1 ± 0.3	43 ± 6	12 ± 1
S9	–	9.1 ± 0.6	8.7 ± 1.1	–	35 ± 5	20 ± 2
S10	0.5 ± 0.08	8.1 ± 0.4	4.6 ± 0.6	2.5 ± 0.3	38 ± 5	15 ± 1
S11	0.3 ± 0.05	4.7 ± 0.3	6.5 ± 0.7	1.9 ± 0.3	40 ± 5	12 ± 1
S12	0.8 ± 0.2	7.9 ± 0.6	7.2 ± 1	1.4 ± 0.5	51 ± 8	16 ± 2
S13	0.7 ± 0.1	4.8 ± 0.4	7.5 ± 0.9	1.6 ± 0.5	50 ± 7	13 ± 1
S14	0.4 ± 0.09	1.4 ± 0.2	8.8 ± 0.9	1.4 ± 0.4	52 ± 7	11 ± 1
S15	0.5 ± 0.1	1.9 ± 0.3	7.7 ± 0.8	1.3 ± 0.3	51 ± 7	11 ± 1
S16	0.5 ± 0.1	3 ± 0.3	7.7 ± 0.9	1.4 ± 0.4	50 ± 7	12 ± 1
S17	2.7 ± 0.5	20 ± 1	6.2 ± 1.3	1 ± 0.5	41 ± 8	10 ± 2
Hectorite SHCa-1(ox)[b]						
S1	0.4 ± 0.09	0.3 ± 0.15	0.5 ± 0.2	1.3 ± 0.3	57 ± 8	12 ± 1
S2	0.3 ± 0.1	0.3 ± 0.15	0.5 ± 0.2	0.8 ± 0.2	60 ± 8	10 ± 1
S3	0.8 ± 0.1	0.4 ± 0.2	0.7 ± 0.3	1.3 ± 0.3	62 ± 9	14 ± 1
S4	0.5 ± 0.1	0.3 ± 0.1	0.4 ± 0.2	1.4 ± 0.3	68 ± 1	1.3 ± 0.3
S5	0.1 ± 0.05	0.1 ± 0.05	–	0.1 ± 0.06	75 ± 9	0.7 ± 0.1
S6	0.4 ± 0.09	0.3 ± 0.15	0.6 ± 0.2	1.5 ± 0.3	57 ± 8	12 ± 1
S7	0.5 ± 0.1	0.3 ± 0.2	6.8 ± 0.8	2.1 ± 0.5	48 ± 7	24 ± 2
S8	0.6 ± 0.1	0.4 ± 0.2	0.7 ± 0.3	2 ± 0.4	49 ± 7	16 ± 1
S9	4 ± 0.8	2 ± 1.1	1 ± 0.5	1.2 ± 0.7	35 ± 11	8.8 ± 1
S10	0.4 ± 0.1	–	1 ± 0.2	0.5 ± 0.2	58 ± 8	9.4 ± 0.8
S11	0.6 ± 0.1	0.2 ± 0.1	–	1.2 ± 0.3	67 ± 9	1.5 ± 0.3
S12	–	0.2 ± 0.1	0.5 ± 0.2	1.3 ± 0.2	65 ± 10	1.2 ± 0.3
S13	0.6 ± 0.1	0.4 ± 0.2	–	1.9 ± 0.3	66 ± 10	3 ± 0.4
S14	0.5 ± 0.1	0.3 ± 0.1	–	1.2 ± 0.3	66 ± 10	3.4 ± 0.4
S15	0.3 ± 0.06	0.2 ± 0.1	–	1.2 ± 0.2	69 ± 8	7 ± 0.6
S16	0.4 ± 0.07	0.3 ± 0.11	–	1.6 ± 0.2	62 ± 8	6.5 ± 0.6
S17	2.1 ± 0.4	0.7 ± 0.4	–	1.7 ± 0.5	49 ± 11	3.6 ± 0.7
S18	0.5 ± 0.08	0.3 ± 0.1	0.3 ± 0.2	1.4 ± 0.2	59 ± 9	3.5 ± 0.4
S19	1 ± 0.2	0.6 ± 0.3	–	3.7 ± 0.7	47 ± 8	23 ± 2
S20	0.8 ± 0.1	0.6 ± 0.3	–	2.1 ± 0.5	45 ± 8	4.4 ± 0.5
S21	0.3 ± 0.06	0.2 ± 0.08	–	1.5 ± 0.2	59 ± 8	10 ± 1
S22	0.3 ± 0.05	0.2 ± 0.1	–	1.4 ± 0.2	63 ± 8	7.9 ± 0.7
S23	0.3 ± 0.06	0.2 ± 0.1	0.4 ± 0.1	1.1 ± 0.2	65 ± 7	11 ± 1
S24	0.2 ± 0.04	0.2 ± 0.07	1 ± 0.2	1.3 ± 0.3	63 ± 7	13 ± 0.3
S25	–	0.3 ± 0.1	0.6 ± 0.2	–	43 ± 6	3.8 ± 0.4
S26	0.3 ± 0.05	0.2 ± 0.1	0.4 ± 0.2	1.1 ± 0.2	67 ± 9	5 ± 0.5
S27	0.4 ± 0.08	0.2 ± 0.1	0.5 ± 0.2	2 ± 0.3	58 ± 8	9.5 ± 0.8
S28	0.2 ± 0.05	0.2 ± 0.09	2.4 ± 0.3	0.9 ± 0.2	53 ± 6	16 ± 1
S29	0.2 ± 0.1	0.2 ± 0.09	0.4 ± 0.2	1.1 ± 0.2	58 ± 7	3.8 ± 0.4
S30	0.3 ± 0.05	0.1 ± 0.07	0.4 ± 0.1	1 ± 0.1	37 ± 5	0.6 ± 0.1
S31	0.7 ± 0.1	0.3 ± 0.1	0.6 ± 0.2	1.8 ± 0.3	60 ± 9	2.5 ± 0.4
S32	0.3 ± 0.06	0.2 ± 0.09	0.4 ± 0.2	1 ± 0.2	62 ± 9	1.9 ± 0.2
Hectorite SHCa-1(an)[c]						
S1	0.7 ± 0.1	–	–	1.7 ± 0.3	52 ± 8	5.3 ± 0.6
S2	0.6 ± 0.1	0.4 ± 0.2	0.3 ± 0.2	1.3 ± 0.3	54 ± 8	5 ± 0.5
S3	0.6 ± 0.1	0.4 ± 0.2	0.4 ± 0.2	2.2 ± 0.4	42 ± 8	1.8 ± 0.3
S4	0.7 ± 0.1	0.4 ± 0.2	0.4 ± 0.3	2.4 ± 0.4	38 ± 8	3.2 ± 0.5

Table 2 (continued)

	As	Fe	Al	S	O	Si
S5	0.5 ± 0.09	–	0.4 ± 0.2	1.9 ± 0.3	43 ± 8	1.1 ± 0.2
S6	0.4 ± 0.09	–	–	1.4 ± 0.2	54 ± 8	3.2 ± 0.4
S7	0.7 ± 0.15	0.3 ± 0.2	–	1.8 ± 0.3	42 ± 8	1.5 ± 0.3
S8	0.7 ± 0.1	–	0.5 ± 0.3	2.4 ± 0.4	39 ± 3	1.7 ± 0.4
S9	0.3 ± 0.05	–	0.3 ± 0.2	1.4 ± 0.2	51 ± 8	0.9 ± 0.2
S10	0.4 ± 0.1	0.2 ± 0.1	0.2 ± 0.2	1.3 ± 0.3	62 ± 9	4.4 ± 0.5
S11	1.3 ± 0.3	1 ± 0.4	0.8 ± 0.5	1.6 ± 0.6	60 ± 10	13 ± 1.6
S12	0.7 ± 0.2	0.5 ± 0.2	0.5 ± 0.4	2.5 ± 0.6	58 ± 9	16 ± 1.5
S13	1 ± 0.3	0.5 ± 0.3	–	1.6 ± 0.5	57 ± 9	15 ± 1.5
S14	1.7 ± 0.4	0.5 ± 0.4	–	2.3 ± 0.7	57 ± 10	18 ± 1.8
S15	1.6 ± 0.4	0.8 ± 0.4	–	1.7 ± 0.7	61 ± 11	14 ± 1.6
S16	2 ± 0.5	0.8 ± 0.4	–	1.2 ± 0.5	64 ± 12	7.5 ± 1.1
S17	0.9 ± 0.2	0.6 ± 0.4	0.6 ± 0.3	3.9 ± 0.7	46 ± 8	33 ± 2.4
S18	0.6 ± 0.1	0.3 ± 0.2	–	1.4 ± 0.3	65 ± 9	6.3 ± 0.7
S19	0.4 ± 0.1	0.4 ± 0.2	–	1.3 ± 0.3	67 ± 10	5.8 ± 0.6
S20	0.2 ± 0.04	0.1 ± 0.06	0.3 ± 0.1	0.7 ± 0.2	60 ± 7	13 ± 1
S21	0.3 ± 0.07	0.2 ± 0.1	–	1 ± 0.2	75 ± 10	4.7 ± 0.5
S22	0.3 ± 0.07	0.2 ± 0.1	0.7 ± 0.2	1.4 ± 0.03	61 ± 7	17 ± 1.4
S23	0.4 ± 0.09	0.3 ± 0.1	0.5 ± 0.2	1.7 ± 0.1	51 ± 7	12 ± 1
S24	0.2 ± 0.04	0.2 ± 0.1	0.2 ± 0.1	0.7 ± 0.2	66 ± 8	2.9 ± 0.3
S25	0.4 ± 0.09	0.2 ± 0.1	0.6 ± 0.2	1 ± 0.3	65 ± 8	12 ± 1
S26	0.4 ± 0.1	0.3 ± 0.2	0.5 ± 0.2	1.3 ± 0.3	67 ± 9	9.8 ± 0.9
S27	0.6 ± 0.1	0.3 ± 0.2	0.5 ± 0.3	1.3 ± 0.3	63 ± 9	6.9 ± 0.7
S28	0.3 ± 0.07	0.2 ± 0.09	0.2 ± 0.1	0.7 ± 0.2	68 ± 8	3.1 ± 0.3
S29	0.6 ± 0.1	0.4 ± 0.2	–	1.3 ± 0.3	63 ± 10	6.7 ± 0.7
S30	1.2 ± 0.4	0.7 ± 0.3	–	0.6 ± 0.4	47 ± 9	9.2 ± 1
S31	0.6 ± 0.1	0.4 ± 0.2	–	1.9 ± 0.4	63 ± 10	6.7 ± 0.7
S32	0.7 ± 0.1	0.8 ± 0.3	0.6 ± 0.2	1.5 ± 0.4	64 ± 10	4.2 ± 0.5
S33	0.4 ± 0.1	0.3 ± 0.2	0.8 ± 0.2	1.5 ± 0.4	55 ± 7	34 ± 2
S34	0.4 ± 0.1	0.2 ± 0.09	0.5 ± 0.2	0.5 ± 0.2	74 ± 10	2.3 ± 0.3
S35	0.8 ± 0.1	0.4 ± 0.2	0.6 ± 0.3	1.9 ± 0.4	61 ± 10	3.4 ± 0.5
S36	0.6 ± 0.1	0.4 ± 0.1	0.4 ± 0.2	1.1 ± 0.3	67 ± 10	7.8 ± 0.7
S37	0.2 ± 0.04	0.2 ± 0.09	–	1.4 ± 0.2	67 ± 8	12 ± 1
S38	0.3 ± 0.06	0.2 ± 0.1	–	1.2 ± 0.3	57 ± 7	24 ± 1.5

[a]Other elements: **S1**: 0.9 ± 0.3%K, 0.7 ± 0.4%Ca; **S2**: 21 ± 7.8%C, 0.7 ± 0.2%Ca; **S3**: 18 ± 6.6%C, 0.6 ± 0.2%Ca; **S4**: 22 ± 7.8%C, 0.9 ± 0.2%Ca; **S5**: 22 ± 8.6%C, 1 ± 0.3%Ca; **S6**: 29 ± 8.3%C; **S7**: 4.5 ± 4.5%C, 1 ± 0.4%Mg, 0.9 ± 0.3%K, 0.8 ± 0.2%Ca, 0.5 ± 0.2%Ti; **S8**: 27 ± 7%C, 0.4 ± 0.3%Mg, 0.5 ± 0.1%Ca; **S9**: 9.3 ± 5.9%C, 7.2 ± 1%Mg, 3 ± 0.4%K, 1 ± 0.3%Ti, 0.2 ± 0.2%V, 0.4 ± 0.2%Co, 0.7 ± 0.4%Ba, 5 ± 0.7%Au; **S10**: 26 ± 7.2%C, 0.3 ± 0.3%Mg, 0.3 ± 0.2%Ca; **S11**: 31 ± 7%C, 0.3 ± 0.2%Mg, 0.5 ± 0.1%Ca, 0.2 ± 0.1%Ti; **S12**: 13 ± 8.7%C, 0.9 ± 0.2%Ca; **S13**: 19 ± 8.2%C, 0.6 ± 0.2%Ca; **S14**: 23 ± 7.5%C, 0.2 ± 0.2%Mg; **S15**: 24 ± 8.5%C; **S16**: 23 ± 8.5%C, 0.4 ± 0.2%Ca; **S17**: 17 ± 10%C, 0.9 ± 0.3%Ca

[b]Other elements: **S1**: 5.4 ± 4%K, 3.9 ± 2.8%N, 1.7 ± 0.5%Na, 7.1 ± 0.9%Mg, 0.2 ± 0.1%K, 8.4 ± 0.5%Ca; **S2**: 7.6 ± 3.8%C, 2.7 ± 2.6%N, 1.6 ± 0.4%Na, 6.9 ± 0.8%Mg; **S3**: 1.8 ± 0.5%Na, 8.3 ± 1%Mg; **S4**: 0.9 ± 0.7%Na, 0.6 ± 0.3%Mg, 0.1 ± 0.08%K, 25 ± 0.8%Ca; **S5**: 7.7 ± 1.9%C, 1.9 ± 1.4%N, 0.7 ± 0.3%Na, 0.4 ± 0.2%Mg, 0.1 ± 0.1%K, 13 ± 0.4%Ca; **S6**: 3.7 ± 3.6%C, 2.1 ± 0.6%Na, 8.6 ± 1%Mg, 12 ± 0.6% Ca, 0.1 ± 0.1%K; **S7**: 4 ± 3.5%N, 4.8 ± 0.9%Na, 3.7 ± 0.6%Mg, 0.3 ± 0.1%K, 2.4 ± 0.3%Ca; **S8**: 8.9 ± 6.4%C, 3.6 ± 3.6%N, 1.6 ± 0.5%Na, 8.2 ± 1%Mg, 0.2 ± 0.15%K, 6.5 ± 0.5%Ca; **S9**: 1.1 ± 0.8%Na, 2.1 ± 0.7%Mg, 0.6 ± 0.6%K, 43 ± 2.5%Ca; **S10**: 18 ± 6.2%C, 1.5 ± 0.5%Na, 6.7 ± 0.8%Mg; **S11**: 3.3 ± 3.2%C, 0.8 ± 0.5%Na, 11 ± 1.3%Mg, 0.1 ± 0.08%K, 13 ± 0.6%Ca; **S12**: 1.7 ± 1.7%C, 0.8 ± 0.7%Na, 1 ± 0.4%Mg, 0.1 ± 0.1%K, 27 ± 0.9%Ca; **S13**: 1 ± 0.75%Na, 2.4 ± 0.2%Mg, 22 ± 0.9%Ca; **S14**: 2.4 ± 2.4%C, 1 ± 0.5%Na, 5.7 ± 0.8%Mg, 17 ± 0.7%Ca; **S15**: 24 ± 8.5%C; **S16**: 6 ± 3.6%C, 1.3 ± 0.4%Na, 9.6 ± 1.1%Mg, 0.1 ± 0.08%K, 9.7 ± 0.5%Ca; **S17**: 6.3 ± 6.3%C, 2.2 ± 2.2%N, 1.3 ± 1.3%Na, 1.1 ± 0.6%Mg, 0.3 ± 0.2%K, 29 ± 1.4%Ca. **S18**: 6.7 ± 3%C, 3.3 ± 3.3%N, 0.1 ± 0.009%K, 20 ± 0.7%Ca; **S19**: 2 ± 0.6%Na, 9.8 ± 1.2%Mg, 0.7 ± 0.3%Cu; **S20**: 0.1 ± 0.1%C, 1.8 ± 1.8%N, 1.8 ± 1.3%F, 0.6 ± 0.6%Na, 2.3 ± 0.5%Mg, 0.2 ± 0.2%K, 36 ± 1.9%Ca; **S21**: 4 ± 3.6%C, 2.5 ± 2.5%N, 3.2 ± 1.1%F, 1.5 ± 0.4%Na, 6.7 ± 0.8%Mg, 0.3 ± 0.18%Ca; **S22**: 6.5 ± 3.4%C, 3.1 ± 2.5%N, 1.3 ± 0.4%Na, 5.8 ± 0.7%Mg, 0.1 ± 0.1%K, 8.6 ± 0.4%Ca, 0.2 ± 0.09%Ca; **S23**: 1.8 ± 0.4%Na, 9.3 ± 1%Mg, 0.1 ± 0.08%K, 4.3 ± 0.2%Ca, 0.2 ± 0.1%Cu; **S24**: 3.6 ± 1.8%N, 2.2 ± 0.4%Na, 9.5 ± 1%Mg, 0.1 ± 0.06%K,

Table 2 (continued)

3.7 ± 0.2%Ca, 0.2 ± 0.09%Cu; **S25**: 37 ± 6.8%C, 1.3 ± 0.9%F, 1.1 ± 0.4%Na, 3.3 ± 0.5%Mg, 6.3 ± 0.4%Ca, 2.3 ± 0.6%Au; **S26**: 5.4 ± 2.9%C, 2.4 ± 2.4%N, 1 ± 0.4%Na, 3.5 ± 0.5%Mg, 0.2 ± 0.1%Cu; **S27**: 1.9 ± 1.9%C, 2.8 ± 2.8%N, 5 ± 1.5%F, 1.5 ± 0.5%Na, 8.6 ± 1%Mg, 0.1 ± 0.09%K, 6.4 ± 0.5%Ca. **S28**: 4.4 ± 3.5%C, 3.1 ± 1.5%N, 4.5 ± 1%F, 2.8 ± 0.5%Na, 8.9 ± 0.9%Mg, 0.2 ± 0.1%K, 1.4 ± 0.1%Ca, 0.2 ± 0.1%Cu; **S29**: 8.4 ± 3%C, 2 ± 1.9%N, 2.3 ± 0.8%F, 1.1 ± 0.3%Na, 11 ± 1.2%Mg, 0.1 ± 0.1%K, 9.4 ± 0.4%Ca; **S30**: 55 ± 8.6%C, 2.8 ± 2.8%N, 0.4 ± 0.3%Na, 0.2 ± 0.1%Mg, 0.1 ± 0.1%K, 0.6 ± 0.1%Ca; **S31**: 1.9 ± 1.9%C, 2.4 ± 2.4%N, 0.6 ± 0.6%Na, 1.6 ± 0.4%Mg, 0.2 ± 0.1%K, 25 ± 0.9%Ca; **S32:** 9.1 ± 2.8%C, 3.7 ± 3.5%N, 1.3 ± 1%F, 1.2 ± 0.3%Mg, 0.1 ± 0.1%K, 17 ± 0.6%Ca

[c]Other elements: **S1**: 20.9 ± 6%C, 2.1 ± 0.4%Mg, 16 ± 0.7%Ca; **S2**: 20 ± 5.3%C, 2.1 ± 0.4%Mg, 14 ± 0.6%Ca; **S3**: 24 ± 6.4%C, 1 ± 0.9%Na, 0.7 ± 0.4%Mg, 25 ± 1%Ca; **S4**: 23 ± 6.8%C, 1.2 ± 0.8%Na, 1.8 ± 0.5%Mg, 25 ± 1%Ca; **S5**: 28 ± 6.1%C, 0.8 ± 0.7%Na, 0.4 ± 0.3%Mg, 21 ± 0.8% Ca; **S6**: 19 ± 5.1%C, 1 ± 0.5%Na, 1.7 ± 0.4%Mg, 16 ± 0.7%Ca; **S7**: 2.7 ± 0.6%Mg, 5.1 ± 0.9%Au, 30 ± 1.7%Ca; **S8**: 23 ± 5.7%C, 28 ± 1%Ca; **S9**: 24 ± 6.6%C, 1 ± 0.7%Na, 0.6 ± 0.5%Mg; **S10**: 29 ± 5.3%C, 0.6 ± 0.4%Na, 0.5 ± 0.3%Mg, 14 ± 0.5%Ca; **S11**: 11 ± 4.8%C, 1.1 ± 0.6%Na, 2.9 ± 0.6%Mg, 14 ± 0.6%Ca; **S12**: 2.4 ± 1.2%Na, 7.5 ± 1.3%Mg, 0.4 ± 0.3%K, 9.2 ± 0.8%Ca; **S13**: 1.9 ± 0.8%Na, 9.4 ± 1.2%Mg, 0.3 ± 0.2%K, 7 ± 0.5%Ca; **S14**: 3.8 ± 2.1%F, 2.5 ± 0.8%Na, 8 ± 1.2%Mg, 0.3 ± 0.2%K, 7.5 ± 0.6%Ca; **S15**: 1.8 ± 0.9%Na, 8.6 ± 1%Mg, 0.4 ± 0.3%K, 7.3 ± 0.7%Ca; **S16**: 1.8 ± 0.9%Na, 6.7 ± 1.2%Mg, 0.5 ± 0.3%K, 9.7 ± 0.8%Ca; **S17**: 2.3 ± 2.3%C, 1.9 ± 1%Na, 3.7 ± 0.9%Mg, 0.4 ± 0.3%K, 14 ± 1%Ca; **S18**: 1.3 ± 0.6%Na, 1.6 ± 0.4%Ca, 0.3 ± 0.3%K, 6 ± 0.6%Ca; **S19**: 1.4 ± 0.6%Na, 3.9 ± 0.7%Mg, 0.2 ± 0.2%K, 18 ± 0.8%Ca; **S20**: 1.7 ± 0.6%Na, 3.6 ± 0.6%Mg, 0.2 ± 0.1%K, 17 ± 0.7%Ca; **S21**: 8.5 ± 3.9%C, 2.5 ± 1.8%N, 1.9 ± 0.4%Na, 10 ± 1%Mg, 0.1 ± 0.07%K, 1.8 ± 0.2%Ca; **S22**: 3.5 ± 0.5%Mg, 0.1 ± 0.07%K, 12 ± 0.5%Ca; **S23**: 2.1 ± 2.1%, 2.4 ± 0.5%Na, 0.1 ± 0.1%K, 11 ± 1.2%Mg, 2.3 ± 0.2%Ca; **S24**: 14 ± 5.9%C, 3.6 ± 3.6%N, 1.5 ± 0.5%Na, 7 ± 0.8%Mg; **S25**: 12 ± 3.4%C, 3.6 ± 2.3%N, 0.9 ± 0.4%Na; 2.5 ± 0.4%Mg; **S26**: 2.7 ± 2.6%N, 2.1 ± 0.5%Na, 8.4 ± 1%Mg, 0.1 ± 0.1%K, 6.6 ± 0.4%Ca; **S27**: 1.5 ± 0.6%Na, 6.6 ± 0.9%Mg, 0.2 ± 0.1%K, 11 ± 0.5%Ca; **S28**: 1.7 ± 0.6%Na, 4.9 ± 0.7%Mg, 0.2 ± 0.2%K, 19 ± 0.8%Ca; **S29**: 11 ± 3.2%C, 3.1 ± 2.3%N, 0.9 ± 0.4%Na, 2.7 ± 0.4%Mg, 0.1 ± 0.08%K, 8.9 ± 0.3%Ca; **S30**: 1.4 ± 0.8%Na, 4 ± 0.2%Mg, 0.1 ± 0.1%K, 20 ± 0.8%Ca; **S31**: 1 ± 0.6%Na, 3.7 ± 0.8%Mg, 0.3 ± 0.2%K, 35 ± 1.5%Ca; **S32**: 1.6 ± 0.7%Na, 3.3 ± 0.6%Mg, 0.2 ± 0.2%K, 21 ± 0.9%Ca; **S33**: 1.2 ± 0.7%Na, 2.6 ± 0.5%Mg, 0.3 ± 0.2%K, 22 ± 0.9%Ca; **S34**: 2.6 ± 2.3%N, 0.9 ± 0.4%Na, 0.8 ± 0.2%Mg, 0.2 ± 0.1%K, 1.4 ± 0.2%Ca; **S35**: 0.8 ± 0.4%Na, 1.3 ± 0.3%Mg, 0.1 ± 0.06%K, 20 ± 0.6%Ca; **S36**: 1.4 ± 0.6%Na, 1.9 ± 0.5%Mg, 0.2 ± 0.1%K, 26 ± 1%Ca; **S37**: 0.8 ± 0.5%Na, 1.4 ± 0.4%Mg, 0.1 ± 0.09%K, 19 ± 0.8%Ca; **S38**: 3.4 ± 2.1%N, 8.5 ± 1%Mg, 2.2 ± 0.5%Na, 0.1 ± 0.07%K, 3.5 ± 0.2%Ca

Surface Fe

Arsenic accumulated in clay minerals; nevertheless, the data show that the values of %As for hectorite (≤ 4% As) could surpass those found in nontronite (≤ 2.7% As; Table 2). Nontronite is an Fe-rich clay mineral [30% (or more) of Fe as Fe_2O_3; Cornell and Schwertmann 2006]; therefore, the total content of structural Fe in the clay mineral per se did not serve as a predictor for the As accumulation. The findings herein expanded on a report showing that Fe in clay minerals guaranteed the preferential retention of As(III) (Ghorbanzadeh et al. 2015).

Surface O

The As accumulation in both clay minerals (hectorite and nontronite) was not related to Si (as Si/O) regardless of dissolved O_2 (Figs. S1 and S2). With that said, As/O vs Si/O graphs showed that the As accumulation (as As/O) occurred at different intervals of Si/O: $0.15 \leq Si/O \leq 0.4$ (nontronite), $0.01 \leq Si/O \leq 0.5$ (hectorite, ox), and $0.01 \leq Si/O \leq 0.7$ (hectorite, an). Consequently, the As accumulation in hectorite occurred in the presence of a higher content of surface O, arguably due to the binding and formation of As-O structural units. In contrast, the As accumulation in nontronite was not limited by its association with surface O.

Factors controlling the accumulation of As in nontronite

Equation 4 shows a positive, shallow relation between As/Fe and Al/Fe in nontronite, which strongly suggested that As was substituted for Fe, similar to Al (Cornell and Schwertmann 2006). Equations 2 and 3 show the significant relations between As/O, Fe/O, As/S and Fe/S in nontronite, which implies that As binds surface O in a similar manner to Fe binding surface O. Finally, a direct comparison of the polynomial coefficients (Eqs. 2 and 3) shows that As was associated with surface O and S, with the former being preferred by a factor of 2:1.

Table 3 Elemental ratios plotted in Figs. 2 and 3

Nontronite NAu-1						Hectorite SHCa-1 (ox)		Hectorite SHCa-1 (an)	
Al/Fe	As/Fe	Fe/O	As/O	Si/O	As/O	Si/O	As/O	Si/O	As/O
0.7	0.1	0.2	0.02	0.3	0.02	0.2	0.01	0.10	0.01
0.5	0.1	0.3	0.01	0.3	0.02	0.2	0.01	0.1	0.01
0.9	0.1	0.1	0.01	0.3	0.01	0.02	0.01	0.04	0.01
0.4	0.1	0.3	0.01	0.4	0.01	0.2	0.01	0.1	0.02
0.5	0.1	0.3	0.02	0.4	0.02	0.5	0.01	0.03	0.01
1.6	0.1	0.1	0.01	0.3	0.01	0.3	0.01	0.1	0.01
0.7	0.1	0.2	0.01	0.4	0.01	0.2	0.1	0.04	0.02
0.9	0.1	0.1	0.01	0.3	0.01	0.02	0.01	0.04	0.02
0.6	0.1	0.2	0.01	0.4	0.01	0.03	0.01	0.02	0.01
1.4	0.1	0.1	0.01	0.3	0.01	0.02	0.01	0.1	0.01
1.6	0.1	0.1	0.01	0.1	0.01	0.1	0.004	0.2	0.02
6.3	0.3	0.03	0.01	0.2	0.01	0.1	0.01	0.3	0.01
4.0	0.3	0.04	0.01	0.2	0.01	0.1	0.04	0.3	0.02
2.6	0.2	0.1	0.01	0.2	0.01	0.1	0.01	0.3	0.03
0.3	0.1	0.5	0.1	0.2	0.1	0.5	0.02	0.2	0.03
						0.1	0.02	0.1	0.03
						0.2	0.005	0.7	0.02
						0.1	0.005	0.1	0.01
						0.2	0.005	0.1	0.01
						0.3	0.005	0.2	0.003
						0.1	0.004	0.1	0.004
						0.2	0.01	0.3	0.005
						0.3	0.004	0.2	0.01
								0.04	0.003
								0.2	0.01
								0.1	0.01
								0.1	0.01
								0.04	0.004
								0.1	0.01
								0.1	0.01
								0.1	0.01
								0.6	0.01
								0.05	0.01
								0.1	0.01
								0.2	0.003
								0.4	0.005

Surface (As)(O)

The association of As(III) with Fe-(hydr)oxides occurs through multiple inner-sphere complexes (Ona-Nguema et al. 2005), outer-sphere complexes and hydrogen bonding interactions, all of which only conform to a weak colligative force. Therefore, in time, a facile detachment of surface As(III) was sought to proceed in hectorite and nontronite.

Surface (As)(S)

The results show that the preferential association of As with S were consistent with evidence that in reducing environments, the solubility of As(III) is limited by sulphide precipitates (Moore et al. 1988). In metal sulphides, adsorbed As(III) becomes incorporated into the mineral lattice (Bostick and Fendorf 2003). This mechanism was

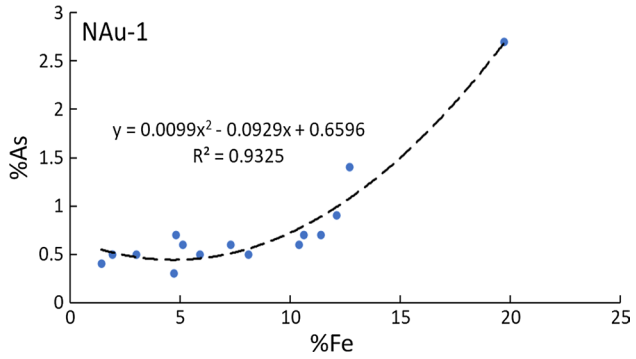

Fig. 2 Relations between %As and %Fe in nontronite

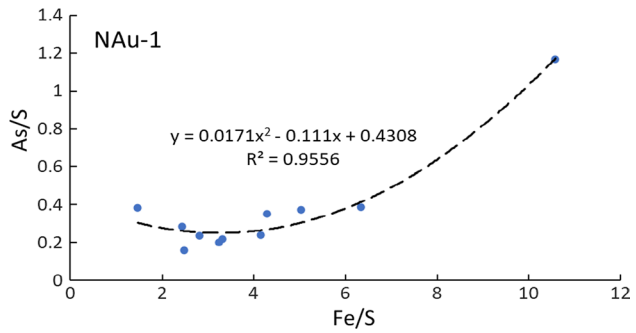

Fig. 3 Relations between As/S and Fe/S in nontronite

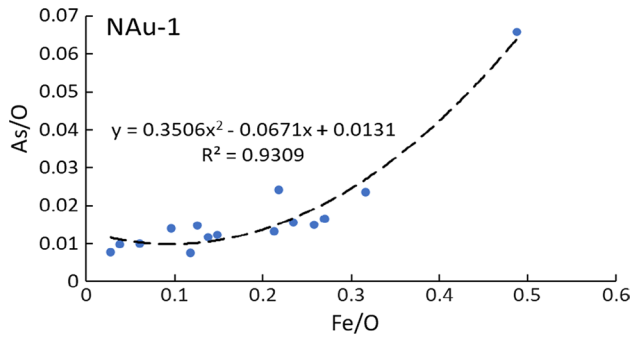

Fig. 4 Relations between As/O and Fe/O in nontronite

responsible for the nonreversible association of As(III) with nontronite surfaces.

Surface (As)(O) and (As)(S)

Reported studies show that minerals determine the mechanism of As adsorption. For example, on pyrite (FeS_2), As strongly binds to form surfaces, inner-sphere complexes with Fe-S ($5 \leq pH$) or ligand exchange with ≡FeOH surface sites (higher pH values). In contrast, on Fe (oxy)hydroxides, anionic As participates in ligand exchange with surface hydroxyl groups

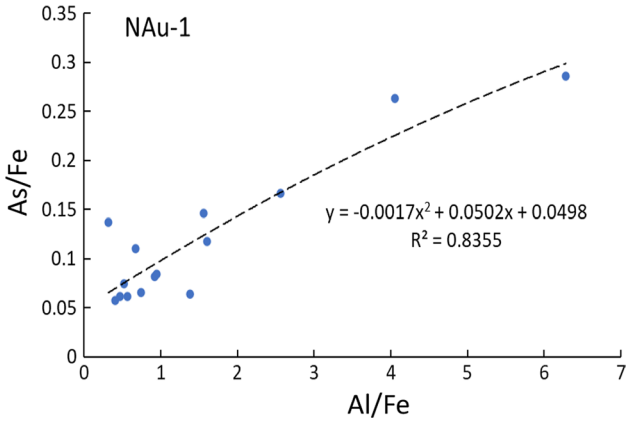

Fig. 5 Relations between As/Fe and Al/Fe in nontronite

(Bonnisel-Gissinger et al. 1998; Bostick and Fendorf 2003; Saunders et al. 2018).

Surface As-ferrihydrite

Mössbauer spectroscopic evidence shows that if anoxic conditions prevailed, the structural (octahedral) Fe of nontronite NAu-1 caused very limited oxidation of adsorbed As(III) (Ilgen et al. 2017). Meanwhile, at circumneutral pH, the dominant As species are $H_2AsO_4^-$ and $HAsO_2^-$ (pKa = 6.9) and $H_3AsO_3^-$ (pKa = 9.2; Fendorf et al. 2010a, b). Thus, in nontronite dispersions, As remained as As(III).

The Fe/As ratio indicates the phases containing As (e.g. Frau et al. 2005; Paktunc et al. 2008). Thus, the obtained As/Fe ratios (Table 3) were used to estimate the corresponding Fe/As ratios, which showed values of $3.3 \leq Fe/As \leq 10$. The obtained Fe/As values were compared to those reported elsewhere (Frau et al. 2005). A study on mine waste materials and stream-bed sediments from the Baccu Locci mine area in Sardinia, Italy, using transmission electron microscopy (TEM) and X-ray photoelectron spectroscopy (XPS) showed Fe/As of 0.9–26 (Frau et al. 2005). There, the registered ratios $Fe/As > 1$ were associated with the formation of ferrisymplesite [$Fe_3(AsO_4)_2(OH)_3 \cdot 5H_2O$], crystalline scorodite [Fe(III) $AsO_4 \cdot 2H_2O$] and arsenical ferrihydrite. Another unrelated study reported the characterization of synthetic scorodite and arsenical ferrihydrite using TEM, X-ray diffraction (XRD) and XANES techniques (Paktunc et al. 2008). Therein, in aqueous dispersions with $1 \leq pH \leq 4.5$ and $1 < Fe/As$, the predominant mineral formed was ferric arsenate, which eventually transformed to scorodite. However, in dispersions with $pH = 4.5$ and $1 \leq Fe/As \leq 4$, the minerals consisted of admixtures of ferric arsenate, arsenical ferrihydrite and As-rich hydrous ferric oxide. If $5 \leq Fe/As$, the growth of ferrihydrite

was favourable, and the two-line ferrihydrite gradually transformed to six-line ferrihydrite. However, ferrihydrite growth was inhibited by As adsorption (Paktunc et al. 2008). Thus, at circumneutral pH, As(III) adsorbed onto nontronite surfaces was concluded to react with surface ferrihydrite to form arsenical ferrihydrite.

Conclusion

This contribution expands on current knowledge on the interaction between As(III) and expandable clay minerals. The higher content of structural Fe in nontronite vs. hectorite favours the retention of As(III). Arguably, adsorbed As(III) on nontronite surfaces (1) transforms to arsenical ferrihydrite or (2) bonds with naturally occurring S; both processes facilitate its nonreversible surface bonding. In addition, adsorbed As(III) on nontronite and hectorite surfaces reversibly bonds to surface O.

Supplementary Information The online version contains supplementary material available at https://doi.org/10.1007/s13762-022-04030-0.

Acknowledgements This research was funded by the National Council of Science and Technology (Consejo Nacional para Ciencia y Tecnología, Mexico, Grant no. 41607).

Author contribution All authors whose names appear on the submission made substantial contributions to the conception of the work, acquisition, analysis, and interpretation of data.

Data availability Data are available upon reasonable request.

Declarations

Conflict of interest The authors declare that they have no conflict of interest.

Human and animal rights The authors declare that no studies performed on humans or animals.

References

Bonnisel-Gissinger P, Alnot M, Ehrhardt J-J, Behra P (1998) Surface oxidation of pyrite as a function of pH. Environ Sci Technol 32:2839–2845. https://doi.org/10.1021/es980213c

Bostick BC, Fendorf S (2003) Arsenite sorption on troilite (FeS) and pyrite (FeS_2). Geochim Cosmochim Acta 67:909–921. https://doi.org/10.1016/S0016-7037(02)01170-5

Chipera SJ, Bish DL (2001) Baseline studies of the clay minerals society source clays: powder X-ray diffraction analyses. Clays Clay Miner 49:398–409. https://doi.org/10.1346/CCMN.2001.0490507

Cornell R Schwertmann U (2006) The iron oxides: structure, properties, reactions, occurrences and uses, 2nd completely revised and extended edn. Wiley-VCH, Weinheim

Devesa V, Del Razo LM, Adair B, Drobna Z, Waters SB, Hughes MF, Stýblo M, Thomas DJ (2004) Comprehensive analysis of arsenic metabolites by pH-specific hydride generation atomic absorption spectrometry. J Anal At Spectrom 19:1460–1467. https://doi.org/10.1039/B407388F

Fendorf S, Nico PS, Kocar BD, Masue Y, Tufano KJ (2010b) Arsenic chemistry in soils and sediments. Dev Soil Sci 34:357–378. https://doi.org/10.1016/S0166-2481(10)34012-8

Fendorf S, Michael HA, van Geen A (2010) Spatial and temporal variations of groundwater arsenic in South and Southeast Asia. Science 328:1123–1127. https://doi.org/10.1126/science.1172974

Frau F, Rossi A, Ardau C, Biddau R, da Pelo S, Atzei D, Licheri C, Cannas C, Capitani GC (2005) Determination of arsenic speciation in complex environmental samples by combined use of TEM and XPS. Microchim Acta 151:189–201. https://doi.org/10.1007/s00604-005-0399-3

Ghorbanzadeh N, Jung W, Halajnia A, Lakzian A, Kanra AN, Jeon B-H (2015) Removal of arsenate and arsenite from aqueous solution by adsorption on clay minerals. Geosystems Engineering 18:302–311. https://doi.org/10.1080/12269328.2015.1062436

Goldberg S (2002) Competitive adsorption of arsenate and arsenite on oxides and clay minerals. Soil Science Society America Journal 66:413–421. https://doi.org/10.2136/sssaj2002.4130

Hernández-Zavala A, Matoŭsek T, Drobná Z, Paul DS, Walton F, Adair BM, Jiří D, Thomas DJ, Stýblo M (2008) Speciation of arsenic in biological matrices by automated hydride generation-cryotrapping-atomic absorption spectrometry with the multiple microflame quartz tube atomizer (multiatomizer. Spectrochim). J Anal At Spectrom 23:342–351. https://doi.org/10.1039/b706144g

Ilgen AG, Kukkadapu RK, Dunphy DR, Artyushkova K, Cerrato JM, Kruichak JN, Janish MT, Sun CJ, Argo JM, Washington RE (2017) Synthesis and characterization of redox-active ferric nontronite. Chem Geol 470:1–12. https://doi.org/10.1016/j.chemgeo.2017.07.010

Keeling J, Raven M, Gates WP (2000) Geology and characterization of two hydrothermal nontronites from weathered metamorphic rocks at the Uley Graphite Mine, South Australia. Clays Clay Miner 48:537–548. https://doi.org/10.1346/CCMN.2000.0480506

Mermut AR, Cano AF (2001) Baseline studies of the clay minerals society source clays: chemical analysis of major elements. Clays Clay Miner 49:381–386. https://doi.org/10.1346/CCMN.2001.0490504

Moore JN, Ficklin WH, Johns C (1988) Partitioning of arsenic and metals in reducing sulfidic sediments. Environ Sci Technol 22:432–437. https://doi.org/10.1021/es00169a011

Moore DM, Reynolds RC Jr (1989) X-ray diffraction and the identification and analysis of clay minerals, 2nd edn. Oxford University Press, Oxford

Ona-Nguema G, Morin G, Juiliot F, Calas G, Brown GEJ (2005) EXAFS analysis of arsenate adsorption onto two-line ferrihydrite, hematite, goethite, and lepidocrocite. Environ Sci Technol 39:9147–9155. https://doi.org/10.1021/es050889p

Paktunc D, Dutrizac J, Gertsman V (2008) Synthesis and phase transformations involving scorodite, ferric arsenate and arsenical ferrihydrite: Implications for arsenic mobility. Geochim Cosmochim Acta 72:2649–2672. https://doi.org/10.1016/j.gca.2008.03.012

Del Razo LM, Stýblo M, Cullen WR, Thomas DJ (2001) Determination of trivalent methylated arsenicals in biological matrices. Toxicol Appl Pharmacol 174:282–293. https://doi.org/10.1006/taap.2001.9226

Saunders J, Lee M-K, Dhakal P (2018) Bioremediation of arsenic-contaminated groundwater by sequestration of arsenic in biogenic pyrite. Appl Geochem 98:233–243. https://doi.org/10.1016/j.apgeochem.2018.07.007

Smedley P, Kinniburgh D (2002) A review of the source, behavior and distribution of arsenic in natural water. Appl Geochem 17:517–568. https://doi.org/10.1016/S0883-2927(02)00018-5

Sparks DL (2003) Environmental soil chemistry. Academic Press, Cambridge

Środoń J, McCarty DK (2008) Surface area and layer charge of smectite from CEC and EGME/H_2O retention measurements. Clays Clay Miner 56:155–174. https://doi.org/10.1346/CCMN.2008.0560203

Sverjensky DA, Fukushi K (2006) A predictive model (ETLM) for As(III) adsorption and surface speciation on oxides consistent with spectroscopic data. Geochim Cosmochim Acta 70:3778–3802. https://doi.org/10.1016/j.gca.2006.05.012